

Rosiglitazone prevents murine hepatic fibrosis induced by *Schistosoma japonicum*

Hui Chen, Yong-Wen He, Wen-Qi Liu, Jing-Hui Zhang

Hui Chen, Yong-Wen He, Department of Infectious Disease, Union Hospital, Tongji Medical College, Huazhong University of Science and Technology, Wuhan 430022, Hubei Province, China
Wen-Qi Liu, Department of Parasitology, Tongji Medical College, Huazhong University of Science and Technology, Wuhan 430022, Hubei Province, China

Jing-Hui Zhang, Department of Surgical Laboratory, Union Hospital, Tongji Medical College, Huazhong University of Science and Technology, Wuhan 430022, Hubei Province, China
Author contributions: Chen H contributed chiefly to this work; Chen H designed and performed the research and wrote the paper; Chen H, Liu WQ and Zhang JH performed the research; He YW gave some good suggestions.

Correspondence to: Hui Chen, Department of Infectious Disease, Union Hospital, Tongji Medical college, Huazhong University of Science and Technology, 1277# Jiefang Road, Wuhan 430022, Hubei Province, China. chenhui0515@yahoo.com.cn
Telephone: +86-27-85726132 Fax: +86-27-85727851
Received: January 25, 2008 Revised: March 8, 2008

Abstract

AIM: To evaluate the effect of rosiglitazone in a murine model of liver fibrosis induced by *Schistosoma japonicum* infection.

METHODS: A total of 50 mice were randomly and averagely divided into groups A, B, C, D and E. The mice in group A served as normal controls, while those in the other four groups were infected with *Schistosoma japonicum* to induce the model of liver fibrosis. Besides, the mice in groups C, D and E were treated with praziquantel, rosiglitazone and praziquantel plus rosiglitazone, respectively. NF- κ B binding activity and expression of PPAR γ -mRNA were determined by Western blot assay and real-time quantitative PCR. Radioimmunoassay technique was used to detect the serum content changes of TNF- α and IL-6. Histological specimens were stained with HE. Expression of TGF- β 1, α -smooth muscle actin and type I and type III collagen was detected by immunohistochemistry and multimedia color pathographic analysis system.

RESULTS: Inflammation and fibrosis in the rosiglitazone plus praziquantel treatment group (group E) were lightest among the mice infected with *Schistosoma* ($P < 0.05$). To further explore the mechanism of rosiglitazone action, we found that rosiglitazone can significantly increase the expression of PPAR γ [E: $-18.212 \pm (-3.909)$ vs B: $-27.315 \pm (-6.348)$ and C: $-25.647 \pm (-5.694)$, $P < 0.05$],

reduce the NF- κ B binding activity (E: 88.89 ± 19.34 vs B: 141.11 ± 15.37 , C: 112.89 ± 20.17 and D: 108.89 ± 20.47 , $P < 0.05$), and lower the serum level of TNF- α (E: 1.613 ± 0.420 ng/mL vs B: 2.892 ± 0.587 ng/mL, C: 2.346 ± 0.371 ng/mL and D: 2.160 ± 0.395 ng/mL, $P < 0.05$) and IL-6 (E: 0.106 ± 0.021 ng/mL vs B: 0.140 ± 0.031 ng/mL and C: 0.137 ± 0.027 ng/mL, $P < 0.05$) in mice with liver fibrosis. Rosiglitazone can also substantially reduce the hepatic expression of TGF- β 1, α -SMA type I and type III collagen in mice with liver fibrosis.

CONCLUSION: The activation of PPAR γ by its ligand can retard liver fibrosis and suggest the use of rosiglitazone for the treatment of liver fibrosis due to *Schistosoma japonicum* infection.

© 2008 WJG. All rights reserved.

Key words: Peroxisome proliferators-activated receptor γ ; Rosiglitazone; Liver fibrosis; Schistosomiasis; Hepatic stellate cell

Peer reviewer: Ana Cristina Simões e Silva, Professor, Pediatrics Department, Federal University of Minas Gerais Institution, Avenida Professor Alfredo Balena, 190, Belo Horizonte 30130-100, Brazil

Chen H, He YW, Liu WQ, Zhang JH. Rosiglitazone prevents murine hepatic fibrosis induced by *Schistosoma japonicum*. *World J Gastroenterol* 2008; 14(18): 2905-2911 Available from: URL: <http://www.wjgnet.com/1007-9327/14/2905.asp> DOI: <http://dx.doi.org/10.3748/wjg.14.2905>

INTRODUCTION

Hepatic schistosomiasis is one of the most prevalent forms of chronic liver diseases in the world, resulting in the morbidity from infection due to its complications of liver fibrosis. However, there are few medicines or means available to control and treat fibrosis in schistosomiasis.

The key pathogenic event in liver fibrosis is the activation of hepatic stellate cells (HSC) and their transformation into myofibroblasts^[1,2]. The HSC (formally called the Ito cell) is the primary cell-type in the liver responsible for excessive collagen synthesis during hepatic fibrosis^[3,4]. Following liver injury, the HSC undergoes a complex transformation or activation process in which the cell changes from a quiescent, vitamin A-storing cell to an

activated myofibroblast, resulting in considerable changes such as the appearance of the cytoskeletal protein smooth muscle α -actin (α -SMA), the loss in the cellular vitamin A stores^[5,6], and the up-regulation of type I and III collagen genes. In addition, transforming growth factor- β (TGF- β), as the most potent fibrogenic cytokine described in HSC^[7], accompanying its receptors are increased following HSC activation as well. These pathogenic alterations cause excessive depositions of extracellular matrix (ECM) proteins including three large families of protein-glycoproteins, collagens and proteoglycans, and disrupt the balance in ECM integrity to induce hepatic fibrosis^[8].

Peroxisome proliferator-activated receptors (PPARs) are a family of ligand-activated nuclear transcription factors, members of the nuclear hormone receptor superfamily^[9]. There are 3 mammalian subtypes identified as PPAR- α , - β (or - δ), and - γ ^[10]; however, current studies demonstrate that only PPAR γ is mainly expressed in human HSC, which contributes to the process of liver fibrogenesis, and both its translational and transcriptional levels are significantly decreased in *in vitro* and/or *in vivo* activated human HSC cells. The decreased PPAR γ at the early stage of HSC activation and the amelioration of stimulated PPAR γ by its ligands to some deterioration resulting from activated HSCs, suggest that PPAR γ may be involved in the maintenance of a quiescent phenotype of HSC^[11], although the identification of PPAR γ as a novel modulator to liver fibrosis remains controversial.

PPAR γ ligands, 15-deoxy-triangle up (1214) prostaglandin J (2) (15d-PGJ (2) and rosiglitazone, significantly decreased the expression of α -SMA and proliferation in activated human HSCs induced by platelet-derived growth factor^[12]. Oral administration of rosiglitazone is found able to diminish extracellular matrix deposition and HSC activation in liver fibrosis of rat models which are created by bile duct ligation^[13]. They found PPAR γ -specific DNA binding activities in nuclear extracts of HSCs isolated from liver fibrotic rat models are impaired significantly, although they can return, through rosiglitazone administration, to the normal levels as controls. Intriguingly, rosiglitazone induces PPAR γ activation to inhibit collagen and fibronectin synthesis in human HSCs initiated by transforming growth factor (TGF)- β 1 *in vitro*. These findings implicate that the PPAR γ activation in HSC retards fibrosis, suggesting the use of PPAR γ ligands for the treatment of fibrosis following liver injury.

To determine amelioration of PPAR γ and its ligands to liver fibrosis, we studied several different treatments of ligands, rosiglitazone, with/out the additives and praziquantel in liver fibrosis model mice created by infection of schistosome.

MATERIALS AND METHODS

Animal preparation and treatment

Fifty 4-5-wk-old Kunming mice, weighing 16-22 g (obtained from the experimental animal center of Tongji Medical College, Huazhong University of Science and Technology) were used. All animals were housed in a temperature and humidity controlled environment, and all

animal experiments were carried out in accordance with the Chinese Council on Animal Care Guide for the Care and Use of Laboratory Animals.

The mice were randomly divided into five groups (10 per group) as follows: group A, B, C, D and E. The mice in group A served as normal controls, while those in the other four groups were infected with 40 *Schistosoma japonicum cercariae* through skin to create a liver fibrosis model. The mice in groups C, D and E were treated with praziquantel, rosiglitazone, and praziquantel plus rosiglitazone, 4 wk after infection, respectively. Praziquantel (500 mg/kg) was given daily for 2 d by intragastric administration in groups C and E. Rosiglitazone (4 mg/kg) was given daily for 6 wk by intragastric administration in groups D and E. Meanwhile, the mice in the normal control group (group A) and the model control group (group B) were given normal saline daily for 6 wk. All mice were sacrificed at the end of the study period. Vein blood was centrifuged at 1500 r/min for 15 min, and the serum was stored at -20°C for use. Parts of liver tissues were fixed by 40 g/L formaldehyde, and embedded in paraffin. The remaining liver was stored at -70°C.

Histopathological examination

The sections of the liver were stained with hematoxylin-eosin (HE) staining. Criteria used in histopathological analysis strictly obeyed WHO category and nomenclature for liver fibrosis^[14]. Mean degrees of liver fibrosis examined from ten randomized scopes under optical microscopy in each slice were used for statistical analysis in current study. Pathological phases are graded as “-”, “+”, “++” and “+++” respectively: “-”, no fibrosis in liver lobules marked phase “0”; “+”, limit fibrosis in lobules, phase “1”; “++”, typical fibrosis spacing around liver lobules, phase “2”; and “+++”, early cirrhosis, fibrosis enveloping liver lobules and spacing into central vein area, phase “3”.

Serum assay

Serum TNF- α and IL-6 were detected using radioimmunoassay kit (Institute of Radioimmunoassay, Science and Technology Empolder Center, General Hospital of PLA) according to the manufacturer's instructions.

Immunohistochemistry for TGF- β , α -SMA and collagens

TGF- β , α -SMA and collagens were detected using the three step streptavidin-biotin immunoperoxidase method. Briefly, tissue sections were de-paraffinized and rehydrated, and then were heated in microwave oven for 10 min to enhance antigen retrieval. For minimizing endogenous peroxidase, activity slides were incubated with 3% H₂O₂. After blocking with 5% normal goat serum in 0.01% PBS, the primary antibodies (mice raised against α -SMA, rabbit raised against TGF- β , and types I and III collagens, Bosider, Wuhan, China) were applied and incubated at 37°C in a moisture chamber for 1 h. Sections were then washed with PBS 3 times. After reacted with biotinylated hircine anti-mouse (or rabbit) IgG and then avidin at 37°C for 20 min each, sections were washed with PBS 3 times. Then diaminobenzidine solution (1 mg/mL in PBS

containing 0.03% hydrogen peroxide) was applied as the chromogen. Sections were counterstained with hematoxylin for 15 s before checked under microscope. As a negative control, PBS was used instead of primary antibody. The cytoplasm or membrane of the positive cell was stained brown and yellow. The sections were observed under microscope. For quantification, 10 random fields of intralobular and periportal areas were evaluated under microscope at 40 × magnification. The integral light density was determined by multimedia color pathographic analysis system.

Protein preparation and western blotting

One hundred mg of frozen tissues was homogenized and centrifuged at 5000 r/min at 4°C for 10 min. The sediment was resuspended in 200 µL of ice-cold extraction buffer A (10 mmol/L HEPES pH 7.9, 1.5 mmol/L MgCl₂, 10 mmol/L KCl, 0.5 mmol/L DTT, 0.5 mmol/L phenylmethylsulfonyl fluoride, 1 µg/mL Aprotinin), and spin down at 5000 r/min at 4°C for 10 min. The sediment was resuspended in 100 µL of extraction buffer C (25% glycerol, 420 mmol/L NaCl, 20 mmol/L HEPES pH 7.9, 1.5 mmol/L MgCl₂, 1% NP40, 0.2 mmol/L EDTA, 0.5 mmol/L DTT, 0.5 mmol/L phenylmethylsulfonyl fluoride, 1 µg/mL each of aprotinin) and kept on ice for 10 min. Finally, it was transferred to a microdosis centrifuge tube and centrifuged at 15000 r/min at 4°C for 20 min. The supernatant was stored at -70°C for use.

Protein concentration was determined using the Coomassie brilliant blue method with G-250 as a standard. Nuclear or cytoplasmic proteins were electrophoresed through 12% SDS-PAGE in Tris-glycine electrophoresis buffer and transferred onto nitrocellulose membrane. The blot was pre-incubated in blocking buffer [Tris buffered saline (TBS) containing Tween and 7% non-fat dried milk powder] at room temperature for 2 h and probed with a primary antibody [rabbit anti-mouse NF-κB polyclonal antibody (Santa Cruz, CA, USA)] at 4°C overnight. After washed three times with 0.1% Tween-TBS, it was incubated with 1:2000 goat anti-rabbit conjugated with horseradish peroxidase (The Eastman Company, Beijing, China) at room temperature for 2 h. Immunoreactive bands were detected by epiluminescence and quantified in arbitrary units [optical density (A) × band area using Vilber Lourmat image analysis system].

RNA isolation, reverse transcription and quantitative PCR

Total RNA was extracted from the frozen liver tissue with Trizol reagent (GIBCO, USA). Complementary DNA (cDNA) was synthesized from total RNA using the reverse transcriptase Superscript II (GIBCO, USA) according to the manufacturer's instructions.

Relative quantification of target gene expression was performed using glyceraldehyde-3-phosphate dehydrogenase (GAPDH) as an internal control. The threshold cycle and the standard curve method were used for calculating the relative amount of the target mRNA. For *PPARγ* mRNA detection, the forward and reverse primers were: 5'-TTTCAAGGGTGCCAGTTTCG-3', and 5'-TCTTTATTCATCAGGGAGGC-3'; for GAPDH, the

primers were: 5'-GATGGTGAAGGTCGGTGTG-3', and 5'-GAGGTCAATGAAGGGGTCG-3'. Real-time PCR was carried out in 50 µL of PCR reaction mixture which contained 1.5 µL of the extracted cDNA, 25 mmol/L MgCl₂, 20 µmol/L each primer, and 1 µL of SYBR Green I (Biotium, USA). A "no template" control was added, which consisted of all the reagents listed above for real-time PCR, except the cDNA template was replaced with water. The following thermal profile was used: 10 min at 94°C, followed by 45 cycles of 94°C for 30 s, 53°C for 30 s, and 72°C for 30 s. Dissociation curve was run to prove the purity of the product.

Data analysis: The relative *PPARγ* mRNA expression levels were calculated by the $\Delta\Delta C_t$ (threshold cycle) method in relation to *PPARγ* expression in the liver tissues. $\Delta\Delta C_t = \Delta C_t$ (specimen) - ΔC_t (GAPDH), $\Delta C_t = C_t$ (negative control) - C_t (specimen). ΔC_t is the relative gene expression (C_t -the number of fractional cycle at which the reporter fluorescence was generated by cleavage of the probe passes a fixed threshold above baseline). The relative difference in expression of the gene of interest and of the internal reference gene is represented by ΔC_t . Changes of gene expression in relation to the calibrator are represented by $2^{\Delta\Delta C_t}$ [relative quantification (RQ)].

Statistical analysis

Means of triplicates were used for statistical analysis by one-way analysis of variance (ANOVA) with post hoc Tukey test for pairwise group comparisons (SPSS 15, SPSS Inc, Chicago, IL, USA). The level of statistical significance was set at 0.05 (two-sided).

RESULTS

Histopathological analysis

Compared with normal mice, slice of the liver from fibrosis model (group B) showed typical damage in the liver lobules: the segregation of liver by collagen fibers, necrosis lesions in the granulomas and inflammatory cells extensively in the periphery of granulomas (Figure 1A). Compared with group B, the decreases were not significant in the fibroplasias, hepatocellular necrosis and inflammatory cell infiltration in the liver slice from groups C and D (fibrosis models treated only with praziquantel or rosiglitazone respectively) (Figure 1B). However, the severity of hepatocellular necrosis and fibroplasias was significantly decreased in the liver of mice treated with praziquantel plus rosiglitazone (group E) compared with group B (Figure 1C). Group E mice also showed thin fibroseptal and decreased inflammatory cell infiltrations in the livers, demonstrating a markedly improved or normal architecture of hepatic lobule.

The pathological phase quantities of groups B, C, D and E were 2.31 ± 0.63 , 1.49 ± 0.77 , 1.38 ± 0.60 and 0.78 ± 0.53 , respectively. Fibrosis in the rosiglitazone plus praziquantel treatment group (group E) was lightest among those with *Schistosoma* infection ($P < 0.05$).

Immunohistochemical findings

TGF-β₁-positive cells were concentrated in the portal

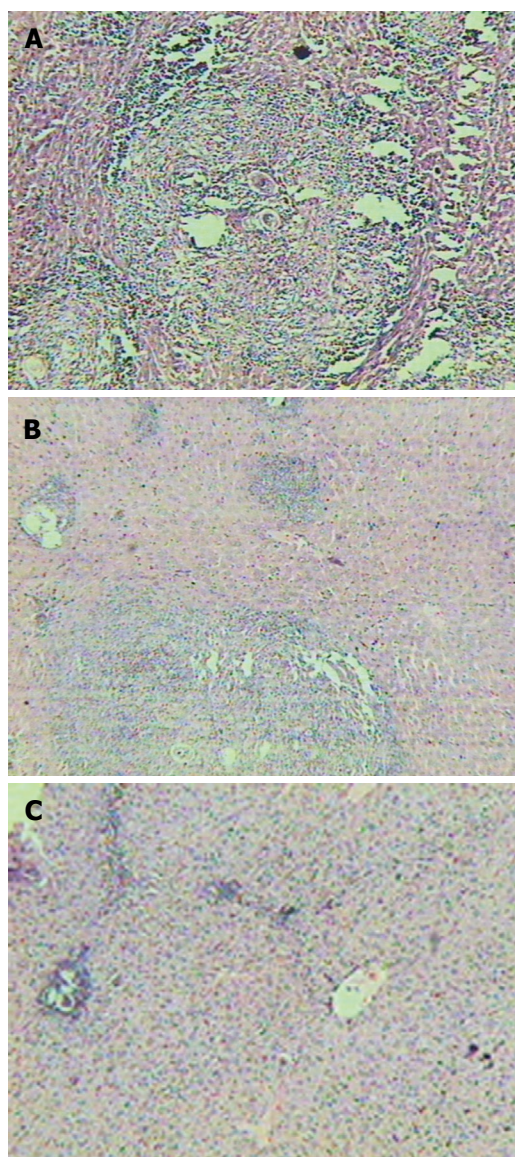


Figure 1 Liver histopathology of mice (HE staining, $\times 10$). **A:** Represents the model group; **B:** Represents the group treated with praziquantel; **C:** Represents the group treated with rosiglitazone plus praziquantel.

venule pericytes with perisinusoidal distribution in the normal mouse liver. Similarly distributed and decreased TGF- β_1 -positive cells were found in group E mice (treated with praziquantel plus rosiglitazone). However, there was a significantly large number of TGF- β_1 -positive cells in groups B, C and D, which distributed mainly at the fibro-septa band, the area of necrosis and inflammatory cell infiltration, few hepatic cells and lipid-containing vacuoles.

There were few expressions of α -SMA positive cells in venule pericytes and periphery of granulomas in the mouse livers of normal control and group E. Nevertheless, the positive cells of α -SMA were substantially distributed at venule pericytes, inflammatory cell infiltration, periphery of granulomas and fibrous proliferation in groups B, C and D.

Moreover, few expressions of type I & III collagen were only found in the central venule pericytes and the linkage region of lobules from the mouse liver of group A (normal control), group D or E. In contrast, there

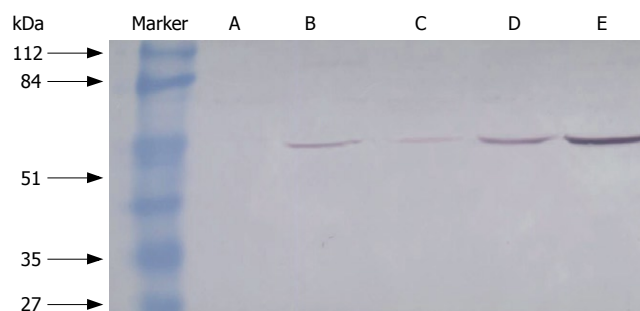


Figure 2 NF- κ B binding activity in mouse livers with Western blot assay. **A:** Normal group; **B:** Rosiglitazone treatment; **C:** Praziquantel plus rosiglitazone treatment; **D:** Praziquantel treatment; **E:** Model group.

was a significant larger number of positive collagen cells distributed not only in these areas but also in fibrous proliferation and Disec cavities of mouse livers from groups B (fibrosis model) and C treated with praziquantel alone.

TGF- β_1 , α -SMA, type I & III collagen positive cells were quantified with multimedia color pathographic analysis. Quantities of TGF- β_1 and type I collagen in the mouse livers of praziquantel treatment group (group C) were reduced much more than in group B ($P < 0.05$). No significant difference was found in the volumes of α -SMA and type III collagen in the mouse livers of groups C and group B ($P > 0.05$). Additionally, volumes of α -SMA and type III collagen in the mouse livers of rosiglitazone treatment group (group D) decreased dramatically compared with groups B and C ($P < 0.05$). TGF- β_1 and type I collagen in mouse livers of group D decreased more significantly than in group B ($P < 0.05$). Notably, volumes of TGF- β_1 , α -SMA, type I & III collagen in the mouse livers of group E (praziquantel plus rosiglitazone treatment) decreased substantially compared to groups B and C as well ($P < 0.05$). All data are summarized in Table 1.

Serum assays

The serum level of TNF- α was markedly lower in group E (1.613 ± 0.420 ng/mL) than that in groups B (2.892 ± 0.587 ng/mL), C (2.346 ± 0.371 ng/mL) and D (2.160 ± 0.395 ng/mL) ($P < 0.05$). However, the serum level of IL-6 was markedly higher in groups B (0.140 ± 0.031 ng/mL), and/or C (0.137 ± 0.027 ng/mL) than that in groups D (0.108 ± 0.021 ng/mL) and/or E (0.106 ± 0.021 ng/mL) ($P < 0.05$) as summarized in Table 2.

NF- κ B binding activity

Less NF- κ B activity was found in groups A, C, D or E than in group B (without any treatment) ($P < 0.05$). Moreover, the activity of NF- κ B decreased much more in group A and E than in either group C or D. The activity of NF- κ B in groups C and D (112.89 ± 20.17 and 108.89 ± 20.47) was higher than in groups A and E (78.89 ± 18.12 , 88.89 ± 19.34 , $P < 0.05$), but lower than in group B (141.11 ± 15.37 , $P < 0.05$). There was no significant difference between groups C and D ($P > 0.05$) as seen in Table 3 and Figure 2.

Table 1 Quantitative analysis of TGF- β 1, α -SMA, type I and type III collagen in mouse livers (mean \pm SD)

Groups	n	TGF- β 1	α -SMA	Type I collagen	Type III collagen
A	10	0.356 \pm 0.145	0.602 \pm 0.116	0.303 \pm 0.117	0.317 \pm 0.133
B	10	0.829 \pm 0.154 ^a	0.915 \pm 0.172 ^a	0.654 \pm 0.186 ^a	0.735 \pm 0.192 ^a
C	10	0.655 \pm 0.117 ^{a,c}	0.902 \pm 0.155 ^a	0.505 \pm 0.103 ^{a,c}	0.701 \pm 0.174 ^a
D	10	0.603 \pm 0.126 ^{a,c}	0.732 \pm 0.109 ^{a,c,e}	0.477 \pm 0.132 ^{a,c}	0.508 \pm 0.127 ^{a,c,e}
E	10	0.459 \pm 0.107 ^{a,c,e,g}	0.689 \pm 0.132 ^{c,e}	0.382 \pm 0.125 ^{c,e,g}	0.436 \pm 0.112 ^{a,c,e}

Compared with group A, ^a*P* < 0.05; Compared with group B, ^c*P* < 0.05; Compared with group C, ^e*P* < 0.05; Compared with group D, ^g*P* < 0.05.

Table 2 Serum level of TNF- α and IL-6 in mice (mean \pm SD)

Groups	n	TNF- α	IL-6
A	10	1.530 \pm 0.380	0.094 \pm 0.026
B	10	2.892 \pm 0.587 ^a	0.140 \pm 0.031 ^a
C	10	2.346 \pm 0.371 ^{a,c}	0.137 \pm 0.027 ^a
D	10	2.160 \pm 0.395 ^{a,c}	0.108 \pm 0.021 ^{c,e}
E	10	1.613 \pm 0.420 ^{c,e,g}	0.106 \pm 0.021 ^{c,e}

Compared with group A, ^a*P* < 0.05; Compared with group B, ^c*P* < 0.05; Compared with group C, ^e*P* < 0.05; Compared with group D, ^g*P* < 0.05.

Table 3 NF- κ B binding activity and the expression of PPAR- γ mRNA in mouse livers (mean \pm SD)

Groups	n	NF- κ B	PPAR- γ mRNA
A	10	78.89 \pm 18.12	-16.557 \pm (-3.022)
B	10	141.11 \pm 15.37 ^a	-27.315 \pm (-6.348) ^a
C	10	112.89 \pm 20.17 ^{a,c}	-25.647 \pm (-5.694) ^a
D	10	108.89 \pm 20.47 ^{a,c}	-18.217 \pm (-4.498) ^{c,e}
E	10	88.89 \pm 19.34 ^{c,e,g}	-18.212 \pm (-3.909) ^{c,e}

Compared with group A, ^a*P* < 0.05; Compared with group B, ^c*P* < 0.05; Compared with group C, ^e*P* < 0.05; Compared with group D, ^g*P* < 0.05.

Expression of PPAR- γ -mRNA

Levels of PPAR γ mRNAs were markedly higher in groups A [-16.557 \pm (-3.022)], D [-18.217 \pm (-4.498)] and E [-18.212 \pm (-3.909)] than that in either group B [-27.315 \pm (-6.348)] or C [-25.647 \pm (-5.694), *P* < 0.05] as summarized in Table 3.

DISCUSSION

PPAR γ is a ligand-activated nuclear transcription factor which belongs to the nuclear hormone receptor superfamily. Normally, PPAR γ expresses in quiescent human liver HSC, but significantly lowers both its translational and transcriptional activities after HSC activation in culture^[15,16]. Some recent findings support a role of PPAR γ in the development of liver fibrosis and suggest that PPAR γ ligands can be therapeutically used to inhibit HSC activation and the progression to liver fibrosis^[17-19].

A mouse model of liver fibrosis through *Japonicum cercariae* infection was generated, and then treated with PPAR γ ligand, rosiglitazone and its additive, and praziquantel to diminish liver fibrosis in the current study. Our results demonstrated that the level of hepatic PPAR γ mRNA markedly decreased in the model mice and praziquantel treated group as compared with the normal mice. However, rosiglitazone significantly increased the expression of PPAR γ and decreased HSC activation and liver fibrosis progression.

Our mouse model successfully showed the key pathogenic events in liver fibrosis: the activation of HSCs and transformation of HSCs into myofibroblasts. Consequently, livers of model mice exhibited cellular changes including the appearance of cytoskeletal protein α -SMA and substantial expression of TGF- β , both fibrogenic cytokines which are activated accompanying

liver HSC activation^[20,21].

Based on the results from histopathological and immunohistochemical analyses, current fibrosis model clearly confirmed that an imbalance between the synthesis and degradation of ECM in chronic liver injury is the indispensable process developing into liver fibrosis. Although there are three large families of ECM proteins, glycoproteins, collagens and proteoglycans^[22,23], excessive depositions of types I and III collagens are mainly pathologic characteristics of liver fibrosis due to *Schistosoma japonicum* infection. Our results further demonstrated that rosiglitazone alone or plus praziquantel can reduce the inflammation and liver fibrosis with *Schistosoma* infection by reducing the hepatic expression of TGF- β 1, α -SMA, types I & III collagens. These results also suggest that PPAR γ ligand, rosiglitazone can impede liver fibrosis after *Schistosoma* infection.

To seek possible regulatory mechanism in liver fibrosis, we further measured some cell factors such as TNF- α and IL-6, and the nuclear factors NF- κ B in our model mice with/out treatment. TNF- α , a pro-inflammatory cytokine, plays a key role in a wide variety of physiological processes, including inflammation, proliferation and programmed cell death^[24] which lead to regeneration of ECM and fibrogenesis^[25]. Our results showed that the serum level of TNF- α and IL-6 increased in liver tissues. These data also provided a further evidence for the role of these cytokines in inducing hepatic fibrosis. Rosiglitazone alone or rosiglitazone plus praziquantel significantly reduced the serum level of TNF- α and IL-6, suggesting that rosiglitazone could be an alternative treatment for liver fibrosis after liver injury or infection.

NF- κ B, a heterodimer, is a functional protein which

is regulated by interaction with a family of regulatory proteins, the inhibitor of nuclear factor κ B (I κ B) proteins may be stimulated by many factors, such as TNF- α and lipopolysaccharide, *via* the phosphorylation and degradation of I κ B. Activated NF- κ B then transports into the cell nucleus and combines with gene promoters to induce the transcription of many cytokines and adhesion molecules^[26,27]. Physical stress, oxidative stress, and exposure to certain chemicals can also activate NF- κ B, suggesting its critical functions in mediating stress responses as well^[28]. Recent studies show that the activation of NF- κ B has a great impact on the pathogenesis of liver fibrosis through regulating hepatocyte, HSC and Kupffer cells^[29,30]. Some studies demonstrate that NF- κ B is also associated with the development of the activated phenotype of HSC and promotes survival of activated HSC^[31] by protecting activated HSCs against TNF-induced apoptosis^[32]. Notably, NF- κ B binding activity increased in our mouse fibrosis model, while rosiglitazone significantly decreased the activity of, suggesting further that rosiglitazone could partially inhibit liver fibrosis by down-regulating NF- κ B as well.

As indicated, our study showed a significant reduction of liver fibrosis following the treatment with rosiglitazone, a PPAR- γ ligand, in a murine model of hepatic fibrosis induced by *Schistosoma japonicum*. The effect of this compound on preventing liver fibrosis may be through down-regulation of liver TGF- β 1 and collagens, and reduction of inflammatory mediators (IL-6, TNF- α , NF- κ B). It suggested the use of rosiglitazone for the treatment of liver fibrosis.

Interestingly, our results showed that praziquantel alone reduced markedly the serum level of TNF- α , NF- κ B binding activity, and volumes of TGF- β 1 and type I collagen in liver fibrosis due to *Schistosoma* infection. These data may suggest an antifibrotic effect of praziquantel in the early stage of liver fibrosis. Praziquantel might be able to block liver fibrosis through killing parasite to alleviate liver inflammation. Further studies on mechanisms of rosiglitazone and praziquantel during liver injury or infection may shed lights on developing therapeutic methods in clinical practice.

COMMENTS

Background

Hepatic schistosomiasis is one of the most prevalent forms of chronic liver diseases in the world, resulting in the morbidity due to its complications of liver fibrosis from infection. However, there are currently few medicines or means available to control and treat fibrosis in schistosomiasis. Many studies demonstrate that PPAR γ is mainly expressed in human HSC and contributes to the process of liver fibrogenesis, but the identification of PPAR γ as a novel modulator to liver fibrosis remains controversial.

Research frontiers

Current findings further support the role of PPAR γ in the development of liver fibrosis and suggest that PPAR γ ligands can be therapeutically used to inhibit HSC activation and the progression of liver fibrosis.

Innovations and breakthroughs

This is a first report about PPAR γ and liver fibrosis due to *Schistosoma* infection. This study evaluates the relationship of PPAR γ ligand and hepatic fibrosis due to *Schistosoma* infection.

Applications

This study provides a perspective for a new therapeutic approach to prevent liver fibrosis following *Schistosoma japonicum* infection.

Peer review

The study reported a significant reduction of liver fibrosis following the treatment with rosiglitazone, a PPAR- γ ligand, in a murine model of hepatic fibrosis induced by *Schistosoma japonicum*. The effect of this compound on preventing liver fibrosis may be through down-regulation of liver TGF- β 1 and collagens, and reduction of inflammatory mediators (IL-6, TNF- α , NF- κ B). The study is interesting and may herald a new therapeutic approach to prevent liver fibrosis following *Schistosoma japonicum* infection.

REFERENCES

- Bartley PB, Ramm GA, Jones MK, Ruddell RG, Li Y, McManus DP. A contributory role for activated hepatic stellate cells in the dynamics of *Schistosoma japonicum* egg-induced fibrosis. *Int J Parasitol* 2006; **36**: 993-1001
- Gutierrez-Ruiz MC, Gomez-Quiroz LE. Liver fibrosis: searching for cell model answers. *Liver Int* 2007; **27**: 434-439
- Parsons CJ, Takashima M, Rippe RA. Molecular mechanisms of hepatic fibrogenesis. *J Gastroenterol Hepatol* 2007; **22** Suppl 1: S79-S84
- Galli A, Svegliati-Baroni G, Ceni E, Milani S, Ridolfi F, Salzano R, Tarocchi M, Grappone C, Pellegrini G, Benedetti A, Surrenti C, Casini A. Oxidative stress stimulates proliferation and invasiveness of hepatic stellate cells via a MMP2-mediated mechanism. *Hepatology* 2005; **41**: 1074-1084
- Zhang XL, Liu JM, Yang CC, Zheng YL, Liu L, Wang ZK, Jiang HQ. Dynamic expression of extracellular signal-regulated kinase in rat liver tissue during hepatic fibrogenesis. *World J Gastroenterol* 2006; **12**: 6376-6381
- Reeves HL, Friedman SL. Activation of hepatic stellate cells-a key issue in liver fibrosis. *Front Biosci* 2002; **7**: d808-d826
- Moreira RK. Hepatic stellate cells and liver fibrosis. *Arch Pathol Lab Med* 2007; **131**: 1728-1734
- Yang C, Zeisberg M, Mosterman B, Sudhakar A, Yerramalla U, Holthaus K, Xu L, Eng F, Afdhal N, Kalluri R. Liver fibrosis: insights into migration of hepatic stellate cells in response to extracellular matrix and growth factors. *Gastroenterology* 2003; **124**: 147-159
- Shearer BG, Hoekstra WJ. Recent advances in peroxisome proliferator-activated receptor science. *Curr Med Chem* 2003; **10**: 267-280
- Berkenstam A, Gustafsson JA. Nuclear receptors and their relevance to diseases related to lipid metabolism. *Curr Opin Pharmacol* 2005; **5**: 171-176
- Marra F, Efsen E, Romanelli RG, Caligiuri A, Pastacaldi S, Batignani G, Bonacchi A, Caporale R, Laffi G, Pinzani M, Gentilini P. Ligands of peroxisome proliferator-activated receptor gamma modulate profibrogenic and proinflammatory actions in hepatic stellate cells. *Gastroenterology* 2000; **119**: 466-478
- Galli A, Crabb D, Price D, Ceni E, Salzano R, Surrenti C, Casini A. Peroxisome proliferator-activated receptor gamma transcriptional regulation is involved in platelet-derived growth factor-induced proliferation of human hepatic stellate cells. *Hepatology* 2000; **31**: 101-108
- Galli A, Crabb DW, Ceni E, Salzano R, Mello T, Svegliati-Baroni G, Ridolfi F, Trozzi L, Surrenti C, Casini A. Antidiabetic thiazolidinediones inhibit collagen synthesis and hepatic stellate cell activation in vivo and in vitro. *Gastroenterology* 2002; **122**: 1924-1940
- Anthony PP, Ishak KG, Nayak NC, Poulsen HE, Scheuer PJ, Sobin LH. The morphology of cirrhosis. Recommendations on definition, nomenclature, and classification by a working group sponsored by the World Health Organization. *J Clin Pathol* 1978; **31**: 395-414
- Yang L, Chan CC, Kwon OS, Liu S, McGhee J, Stimpson SA, Chen LZ, Harrington WW, Symonds WT, Rockey DC. Regulation of peroxisome proliferator-activated receptor-

- gamma in liver fibrosis. *Am J Physiol Gastrointest Liver Physiol* 2006; **291**: G902-G911
- 16 **Guo YT**, Leng XS, Li T, Peng JR, Song SH, Xiong LF, Qin ZZ. Effect of ligand of peroxisome proliferator-activated receptor gamma on the biological characters of hepatic stellate cells. *World J Gastroenterol* 2005; **11**: 4735-4739
 - 17 **Kawaguchi K**, Sakaida I, Tsuchiya M, Omori K, Takami T, Okita K. Pioglitazone prevents hepatic steatosis, fibrosis, and enzyme-altered lesions in rat liver cirrhosis induced by a choline-deficient L-amino acid-defined diet. *Biochem Biophys Res Commun* 2004; **315**: 187-195
 - 18 **Marra F**, DeFranco R, Robino G, Novo E, Efsen E, Pastacaldi S, Zamara E, Vercelli A, Lottini B, Spirli C, Strazzabosco M, Pinzani M, Parola M. Thiazolidinedione treatment inhibits bile duct proliferation and fibrosis in a rat model of chronic cholestasis. *World J Gastroenterol* 2005; **11**: 4931-4938
 - 19 **Zhao C**, Chen W, Yang L, Chen L, Stimpson SA, Diehl AM. PPARgamma agonists prevent TGFbeta1/Smad3-signaling in human hepatic stellate cells. *Biochem Biophys Res Commun* 2006; **350**: 385-391
 - 20 **Jiang W**, Yang CQ, Liu WB, Wang YQ, He BM, Wang JY. Blockage of transforming growth factor beta receptors prevents progression of pig serum-induced rat liver fibrosis. *World J Gastroenterol* 2004; **10**: 1634-1638
 - 21 **Kershenovich Stalnikowitz D**, Weissbrod AB. Liver fibrosis and inflammation. A review. *Ann Hepatol* 2003; **2**: 159-163
 - 22 **Tsukada S**, Parsons CJ, Rippe RA. Mechanisms of liver fibrosis. *Clin Chim Acta* 2006; **364**: 33-60
 - 23 **Benyon RC**, Arthur MJ. Extracellular matrix degradation and the role of hepatic stellate cells. *Semin Liver Dis* 2001; **21**: 373-384
 - 24 **Theiss AL**, Simmons JG, Jobin C, Lund PK. Tumor necrosis factor (TNF) alpha increases collagen accumulation and proliferation in intestinal myofibroblasts via TNF receptor 2. *J Biol Chem* 2005; **280**: 36099-36109
 - 25 **Simeonova PP**, Gallucci RM, Hulderman T, Wilson R, Kommineni C, Rao M, Luster MI. The role of tumor necrosis factor-alpha in liver toxicity, inflammation, and fibrosis induced by carbon tetrachloride. *Toxicol Appl Pharmacol* 2001; **177**: 112-120
 - 26 **Cogswell PC**, Kashatus DF, Keifer JA, Guttridge DC, Reuther JY, Bristow C, Roy S, Nicholson DW, Baldwin AS Jr. NF-kappa B and I kappa B alpha are found in the mitochondria. Evidence for regulation of mitochondrial gene expression by NF-kappa B. *J Biol Chem* 2003; **278**: 2963-2968
 - 27 **Lawrence T**, Bebie M, Liu GY, Nizet V, Karin M. IKKalpha limits macrophage NF-kappaB activation and contributes to the resolution of inflammation. *Nature* 2005; **434**: 1138-1143
 - 28 **Li X**, Stark GR. NFkappaB-dependent signaling pathways. *Exp Hematol* 2002; **30**: 285-296
 - 29 **Mann DA**, Smart DE. Transcriptional regulation of hepatic stellate cell activation. *Gut* 2002; **50**: 891-896
 - 30 **Smart DE**, Vincent KJ, Arthur MJ, Eickelberg O, Castellazzi M, Mann J, Mann DA. JunD regulates transcription of the tissue inhibitor of metalloproteinases-1 and interleukin-6 genes in activated hepatic stellate cells. *J Biol Chem* 2001; **276**: 24414-24421
 - 31 **Muhlbauer M**, Weiss TS, Thasler WE, Gelbmann CM, Schnabl B, Scholmerich J, Hellerbrand C. LPS-mediated NFkappaB activation varies between activated human hepatic stellate cells from different donors. *Biochem Biophys Res Commun* 2004; **325**: 191-197
 - 32 **Elsharkawy AM**, Oakley F, Mann DA. The role and regulation of hepatic stellate cell apoptosis in reversal of liver fibrosis. *Apoptosis* 2005; **10**: 927-939

S- Editor Li DL L- Editor Ma JY E- Editor Yin DH